International Journal on Magnetic Particle Imaging
Vol 6, No 2, Suppl 1, Article ID 2009030, 3 Pages

Infinite Science Publishing

Proceedings Article

Reducing displacement artifacts by warping system matrices in efficient joint multi-patch magnetic particle imaging

M. Boberg[1,2,*] · T. Knopp[1,2] · M. Möddel[1,2]

[1]Section for Biomedical Imaging, University Medical Center Hamburg-Eppendorf, Hamburg, Germany
[2]Institute for Biomedical Imaging, Hamburg University of Technology, Hamburg, Germany
[*]Corresponding author, email: m.boberg@uke.de

Abstract

The reconstruction of multi-patch magnetic particle imaging data requires a compromise between image quality and calibration time. While optimal image quality is ensured by the joint reconstruction approach, a system matrix needs to be acquired for each patch. One can reuse system matrices by shifting them in space, which decreases the calibration effort but leads to distortions due to field imperfections. In this work, we introduce a method for reducing displacement artifacts in the efficient joint multi-patch reconstruction. Based on the magnetic fields we propose a mapping that warps the central system matrix to capture the spatial displacement of off-center system matrices. In this way, we can maintain the low calibration time while significantly improving the image quality.

I Introduction

In magnetic particle imaging (MPI) the field of view is limited due to peripheral nerve stimulation and specific absorption rates. Multi-patch imaging sequences can be used to bypass this limitation [1]. However, the joint reconstruction of Fourier domain data requires a system matrix for each patch [2]. While this provides optimal image quality the calibration and reconstruction are time-consuming. Reusing only a single system matrix speeds up the calibration and reconstruction, but leads to displacement artifacts due to field imperfections [3]. In this abstract, we present a method to reduce these artifacts, where we not only take the spatial shift into account [3] but also the non-linear displacement of the system matrix.

II Material and methods

We consider a multi-patch imaging sequence with L patches characterized by the field-free-point (FFP) $\xi_l \in \mathbb{R}^3$, $l = 1,\dots,L$ of the underlying selection and focus field. In [3], a translation $\mathbf{T}^{\xi}: \mathbb{R}^3 \to \mathbb{R}^3$, $\mathbf{r} \mapsto \mathbf{r}+\xi$ is used to obtain each system function from the function $\hat{\mathbf{s}}^0$ measured in the center by $\hat{\mathbf{s}}^l(\mathbf{r}) \approx \hat{\mathbf{s}}^0(\mathbf{T}^{-\xi_l}(\mathbf{r}))$. Here, $\hat{\mathbf{s}}^l : \Omega_l \to \mathbb{C}^K$ denotes the Fourier transformed system function that maps from $\Omega_l = \text{supp}(\hat{\mathbf{s}}^l) \subseteq \mathbb{R}^3$ to K frequency components. To further reduce image artifacts, we replace the translation $\mathbf{T}^{-\xi_l}$ by a more general non-rigid transformation $\varphi_l : \Omega_l \to \Omega_0$ yielding

$$\hat{\mathbf{s}}^l(\mathbf{r}) \approx \hat{\mathbf{s}}^0(\varphi_l(\mathbf{r})). \tag{1}$$

For instance, φ_l can be obtained by image registration techniques if the system matrices are available. Since the goal is to reduce the calibration effort, we use a different approach and calculate φ_l without calibration of

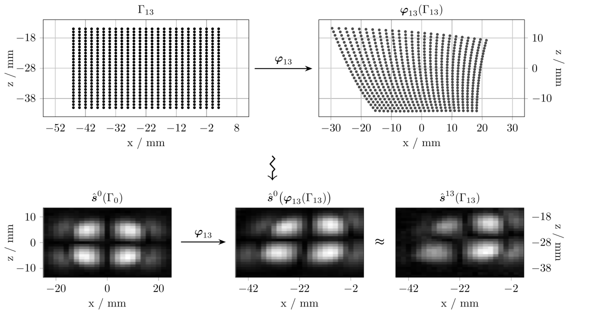

Figure 1: Visualization of the mapping φ and the resulting system matrix for patch 13. In the upper part, the sampling positions of system matrix $\hat{\mathbf{s}}^{13}$ are shown on the left side. Applying the mapping φ_{13} to Γ_{13} yields the positions on the right side. Sampling $\hat{\mathbf{s}}^{0}$ at $\varphi_{13}(\Gamma_{13})$ yields an approximation of $\hat{\mathbf{s}}^{13}$ as shown below for the 1733th frequency component.

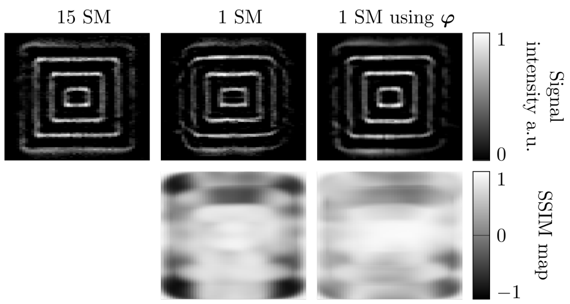

Figure 2: Comparison of different reconstruction methods. In the first row, one slice of the reconstructed 3D tomogram is shown. On the left, the joint reconstruction approach is used while the efficient joint reconstruction approach is used in the center. On the right, the reconstruction with our approach is visualized. Below, the structured similarity (SSIM) map is shown comparing the reconstructions above with the joint approach.

the other system matrices and take the magnetic fields

$$\mathbf{H}^l(\mathbf{r},\mathbf{I}) = \mathbf{H}_{SF}^{\xi_l}(\mathbf{r}) + \sum_{q=1}^{Q} \mathbf{p}_{DF}^{q}(\mathbf{r}) I^q \quad (2)$$

into account, which are the main cause for spatial distortions of the system matrices. The total magnetic field $\mathbf{H}^l : \mathbb{R}^3 \times \mathbb{R} \to \mathbb{R}^3$ of the l-th patch is a superposition of the static selection and focus field $\mathbf{H}_{SF}^{\xi_l} : \mathbb{R}^3 \to \mathbb{R}^3$ with FFP at ξ_l and the Q drive-field coil sensitivities $\mathbf{p}_{DF}^{q} : \mathbb{R}^3 \to \mathbb{R}^3$ multiplied with the currents $\mathbf{I} \in \mathbb{R}^Q$, where $\mathbf{r} \in \mathbb{R}^3$ describes the spatial position.

Each system function $\hat{\mathbf{s}}^l$ maps spatial positions $\mathbf{r} \in \Omega_l$ to the respective MPI signal obtained from an MPI tracer at this location during excitation with dynamic currents. The most significant signal contributions are generated when the FFP traverses $\mathbf{r}$, i.e. when the magnetic field $\mathbf{H}^l(\mathbf{r},\mathbf{I})$ is small. Using this observation we propose to approximate $\hat{\mathbf{s}}^l(\mathbf{r}) \approx \hat{\mathbf{s}}^0(\tilde{\mathbf{r}})$ if a current vector $\mathbf{I}$ exists satisfying $\mathbf{H}^l(\mathbf{r},\mathbf{I}) = \mathbf{H}^0(\tilde{\mathbf{r}},\mathbf{I}) = 0$. The mapping from $\mathbf{r}$ to $\tilde{\mathbf{r}}$ defines our desired mapping φ_l and can be calculated in the following steps for each $l = 1,\ldots,L$.

1. Using Eq. (2) the applied currents $\mathbf{I}$ for each sample position of the system function can be calculated by solving $\mathbf{H}^l(\mathbf{r},\mathbf{I}) = 0$ for all $\mathbf{r} \in \Omega_l$.
2. The corresponding FFP positions $\tilde{\mathbf{r}}$ of the central system function are obtained by solving $\mathbf{H}^0(\tilde{\mathbf{r}},\mathbf{I}) = 0$ for each current calculated in the first step.

In practice, the sampling positions are a discrete set of equidistant points $\Gamma_l \subseteq \Omega_l$, as shown in the upper left part of Fig. 1. Calculating the corresponding points with the two steps above for an exemplary system matrix yields in the positions on the upper right side. In general, they do not coincide with the equidistant sampling grid of the central system matrix, why an additional inter- and extrapolation is necessary.

III Results and discussion

The method is tested on a multi-patch dataset with $L = 15$ patches at different patch positions in the xz-plane including the central patch covering a phantom of size 82×76 mm^2 [3]. The selection-field gradient is set to 1.5 Tm^{-12} in z-direction and -0.75 Tm^{-1} in x- and y-directions. The amplitudes of all three drive fields are set to 12 mT. The fields were measured with a Hall sensor respectively calibration coils [4].

Measuring one system matrix took 8.5 hours, giving a total measurement time of 6 days for all 15 system matrices. The computation of all φ_l took a few seconds for step 1 and about 15 minutes for step 2. An upper bound for the computation of all off-center system matrices with linear interpolation of the central system matrix is 10 minutes for 5104 frequency components. Although some optimizations should still be made, the total time of about 9 hours is much less than 6 days for a complete measurement.

The warped system matrices have in common that the displacement caused by the magnetic fields is well modeled by our method as shown in Fig. 1 for the 13th patch and 1733th frequency component. However, our mapping does not capture spatial intensity variations, which needs further investigations. To avoid extrapolation in the calculation step of φ_l the sampling grid of the central system matrix should be larger, so that the convex hull of $\varphi_l(\Gamma_l)$ is a subset of Γ_0 for all patches. The small increase of calibration time should be compensated by the gain in image quality.

Reconstruction results are shown in the first row of Fig. 2. In each image one xz-slice of the 3D image is shown. As ground truth, the joint reconstruction [2] performed with all 15 measured system matrices is shown on the left. In the middle, the efficient approach [3] using only the central system matrix is shown. The reconstruction result of our proposed method is visualized on the right. It is clearly visible that the rectangular shape of the phantom is better preserved than in the reconstruction with the efficient approach. For comparison, the structured similarity (SSIM) map [5] is shown in the second row. It visualizes the differences between the reconstructed image above with the joint approach. An SSIM index of 1 signifies a perfect match while negative values indicate a locally inverted image. It is obvious that the error in the reconstruction using our proposed method is much lower. The mean SSIM index of 0.79 for our method and 0.69 for the efficient approach shows that the image quality improved significantly.

IV Conclusions

In this work, we introduced a method to reduce displacement artifacts in efficient joint multi-patch reconstructions. With our magnetic-field based mapping the spatial structure of off-center system matrices can be accurately approximated. This yields better reconstruction results than the efficient joint approach, while maintaining the fast calibration time of this approach. Our method can be particularly valuable where accurate localization is required, such as when navigating catheters or other medical devices.

Author's Statement

Research funding: The authors thankfully acknowledge the financial support by the German Research Foundation (DFG, grant number KN 1108/2-1) and the Federal Ministry of Education and Research (BMBF, grant number 05M16GKA). Conflict of interest: Authors state no conflict of interest. Informed consent: Informed consent has been obtained from all individuals included in this study.

References

[1] B. Gleich and J.Weizenecker. Tomographic imaging using the nonlinear response of magnetic particles. Nature, 435(7046):1214–1217, June 2005.

[2] T. Knopp, K. Them, M. Kaul, and N. Gdaniec. Joint reconstruction of non-overlapping magnetic particle imaging focus-field data. Physics in Medicine and Biology, 60:L15, 2015. doi: 10.1088/0031-9155/60/8/L15.

[3] P. Szwargulski, M. Möddel, N. Gdaniec, and T. Knopp. Efficient Joint Image Reconstruction of Multi-Patch Data reusing a Single System Matrix in Magnetic Particle Imaging. IEEE Transactions on Medical Imaging, 38(4):932–944, 2019.

[4] M. Boberg, T. Knopp, and M.Möddel. Analysis and Comparison of Magnetic Fields in MPI using Spherical Harmonic Expansions. Book of Abstracts IWMPI, pages 159–160, 2017.

[5] D. Brunet, E. R. Vrscay, and Z.Wang. On the mathematical properties of the structural similarity index. IEEE Transactions on Image Processing, 21(4):1488–1499, 2012.

10.18416/ijmpi.2020.2009030